

Glenn  
Myers

David  
Ceddia

Imants  
Svalbe

Alexander  
Rack

Andrew  
Kingston

Timur  
Gureyev

Daniele  
Pelliccia

Valentina  
Cantelli

Filomena  
Salvemini

Mario  
Scheel

Ulf  
Garbe

Alex  
Kozlov

Yin  
Cheng

Joseph  
Bevitt

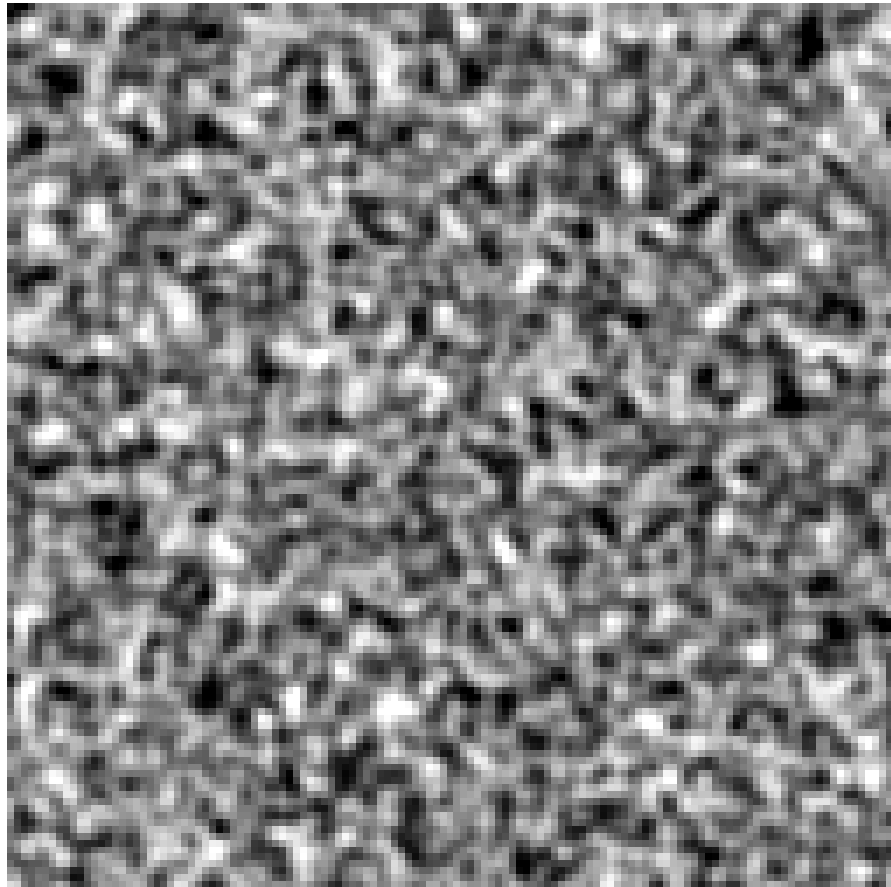
Margie  
Olbinado

David  
Paganin

Harry  
Quiney

# Ghost imaging using x rays and neutrons

# Speckles





Ceddia & Paganin, Phys. Rev. A **97**, 062119 (2018).

Gureyev, Paganin, Kozlov, Nesterets, Quiney, Phys. Rev. A **97**, 053819 (2018).

# “Building signals out of noise”

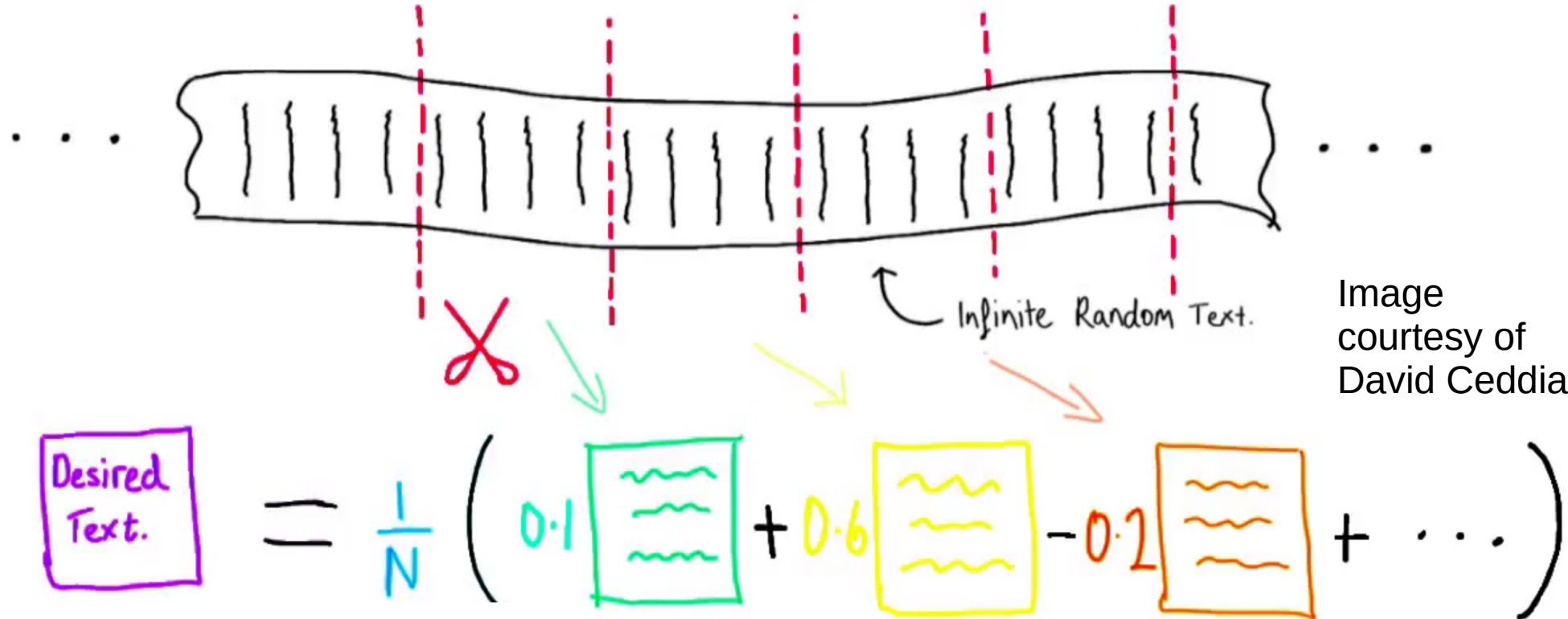


Image  
courtesy of  
David Ceddia

Ceddia & Paganin, Phys. Rev. A **97**, 062119 (2018).

Gureyev, Paganin, Kozlov, Nesterets, Quiney, Phys. Rev. A **97**, 053819 (2018).

$$\begin{matrix} \text{Image of a handwritten digit} \\ = a \end{matrix} \begin{matrix} \text{Image of vertical bars} \\ + b \end{matrix} \begin{matrix} \text{Image of diagonal bars} \\ + c \end{matrix} \begin{matrix} \text{Image of horizontal bars} \\ + d \end{matrix} \begin{matrix} \text{Image of vertical bars} \\ + \dots \end{matrix}$$

5

# “Building signals out of noise”

6

$$\begin{matrix} \text{Image} \\ = a \\ + b \\ + c \\ + d \\ + \dots \end{matrix}$$

The diagram illustrates the decomposition of a grayscale image of a skull into a sum of components. On the left, a black-and-white image of a skull is shown within a thick black rectangular frame. To its right is an equals sign (=). Following the equals sign are four terms, each consisting of a grayscale image followed by a label: 'a', 'b', 'c', and 'd'. Below these four terms is a plus sign (+). To the right of the plus sign is a final term consisting of three dots (...).

Pelliccia, Olbinado, Rack, Kingston, Myers & Paganin, IUCrJ 5, 428 (2018)  
Ceddia & Paganin, Phys. Rev. A. 97 062119 (2018)

$$\{\epsilon N_j(x)\} \quad j = 1, \dots, m$$

$$\uparrow \epsilon N_j(x)$$

~~$$x$$~~

$$\epsilon N_j(x) \equiv I_j(x) - \bar{I}$$

$$\frac{1}{m} \sum_{j=1}^m \epsilon N_j(x) \epsilon N_j(x') = \Delta(x-x')$$

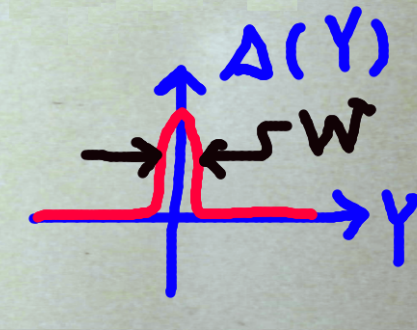
cf.  $\delta(x)$

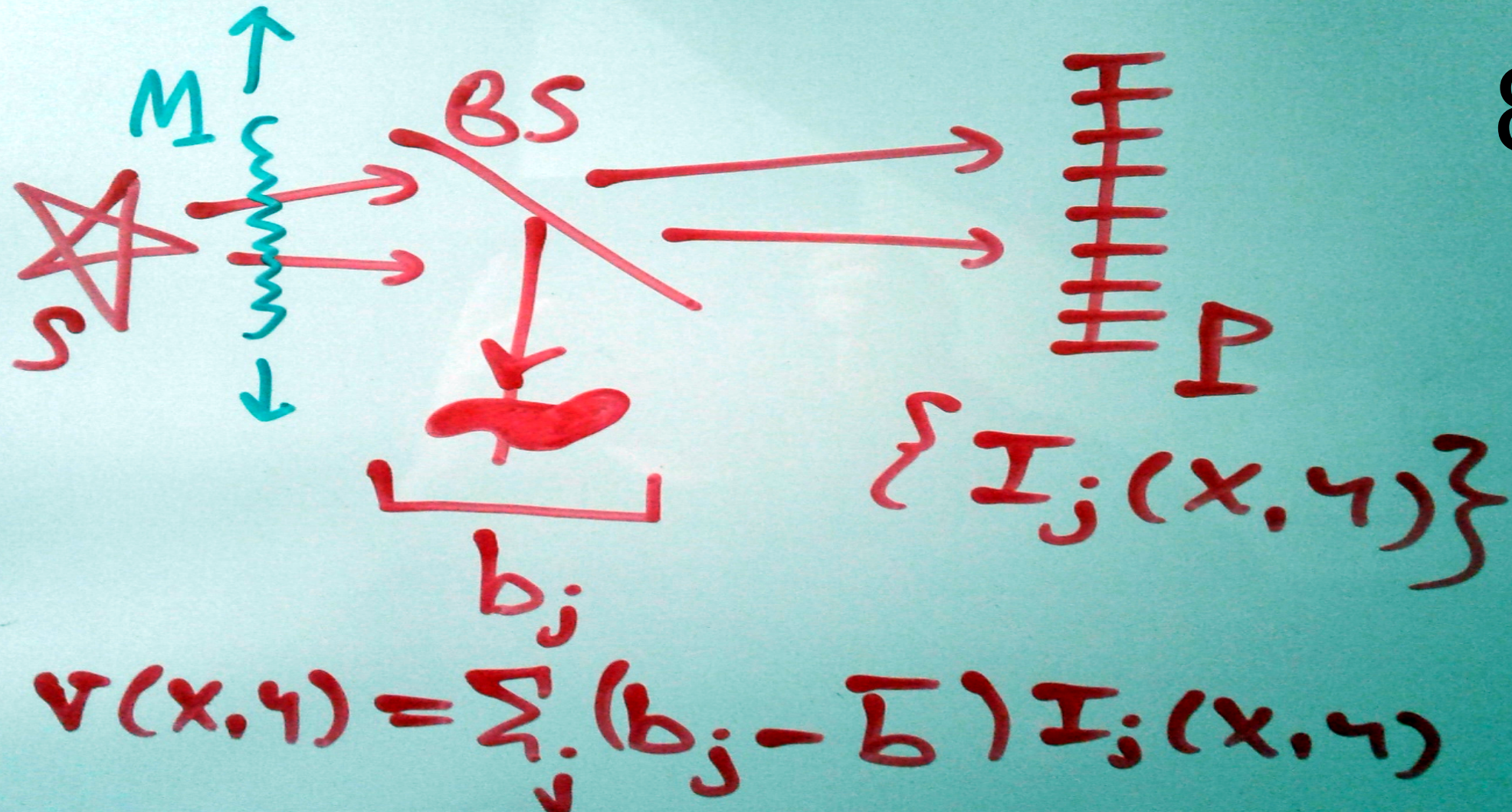
$$\frac{1}{m} \sum_{j=1}^m \epsilon N_j(x) \left[ \int_x^{x'} \epsilon N_j(x') v(x') dx' \right] = \int \Delta(x-x') v(x') dx'$$

$$\langle \epsilon N_j(x), v(x) \rangle \equiv v_j$$

7

$$\frac{1}{m} \sum_{j=1}^m \epsilon N_j(x) v_j = v(x) \otimes \Delta(x)$$





Bromberg, Katz and Silberberg, Phys. Rev. A, 79, 053840 (2009).



## Fourier-Transform Ghost Imaging with Hard X Rays

Hong Yu,<sup>1</sup> Ronghua Lu,<sup>1</sup> Shensheng Han,<sup>1,\*</sup> Honglan Xie,<sup>2</sup> Guohao Du,<sup>2</sup> Tiqiao Xiao,<sup>2</sup> and Daming Zhu<sup>3,4</sup>

<sup>1</sup>*Key Laboratory for Quantum Optics and Centre for Cold Atom Physics, Shanghai Institute of Optics and Fine Mechanics, Chinese Academy of Sciences, Shanghai 201800, China*

<sup>2</sup>*Shanghai Institute of Applied Physics, Chinese Academy of Sciences, Shanghai 201800, China*

<sup>3</sup>*University of Science and Technology of China, Hefei 230026, China*

<sup>4</sup>*University of Missouri-Kansas City, Kansas City, Missouri 64110, USA*

(Received 13 May 2016; published 7 September 2016)



## Experimental X-Ray Ghost Imaging

Daniele Pelliccia,<sup>1,2,3,\*</sup> Alexander Rack,<sup>4</sup> Mario Scheel,<sup>5</sup> Valentina Cantelli,<sup>6,4</sup> and David M. Paganin<sup>3</sup>

<sup>1</sup>*School of Science, RMIT University, Victoria 3001, Australia*

<sup>2</sup>*Australian Synchrotron, Victoria 3168, Australia*

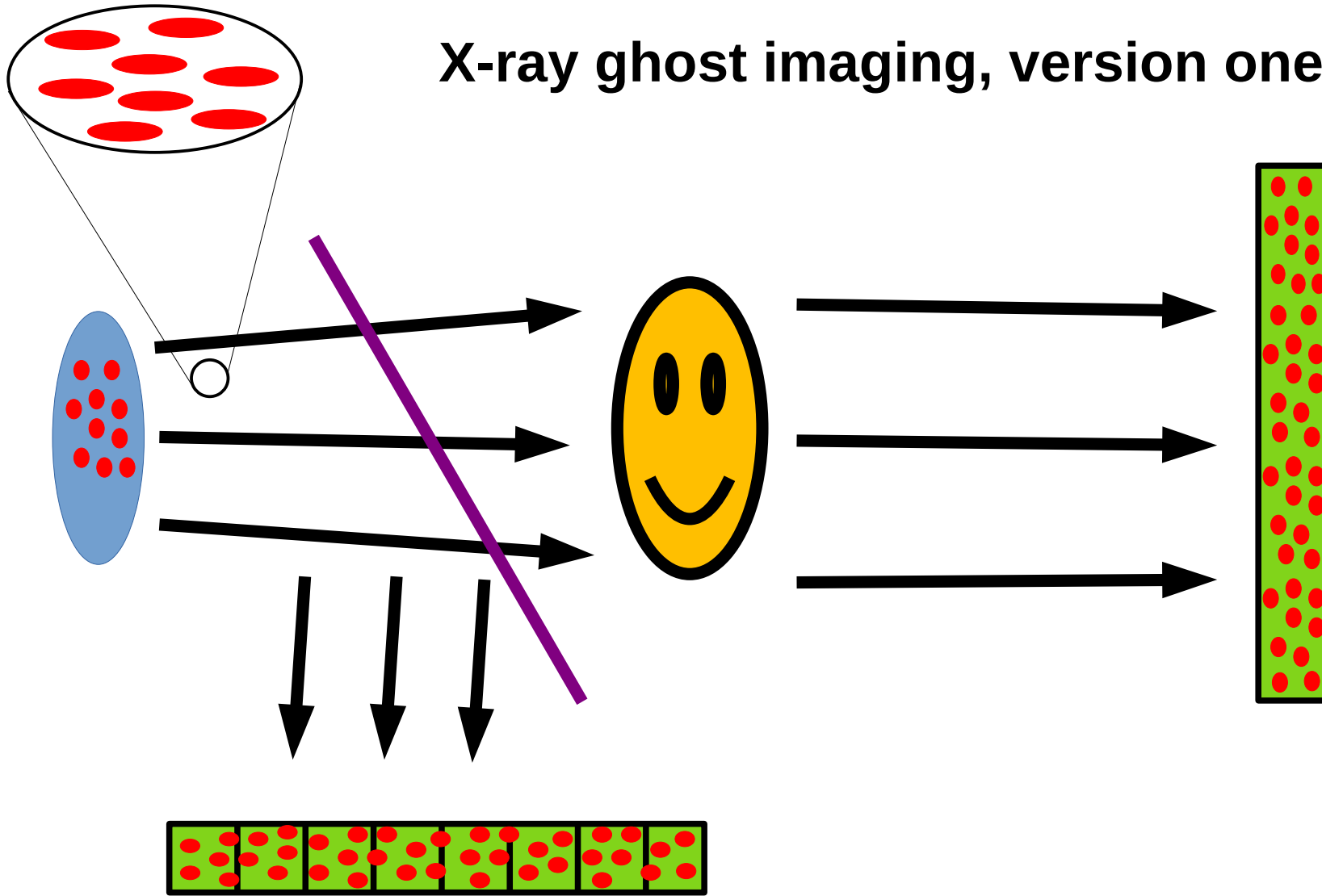
<sup>3</sup>*School of Physics and Astronomy, Monash University, Victoria 3800, Australia*

<sup>4</sup>*European Synchrotron Radiation Facility, 38043 Grenoble, France*

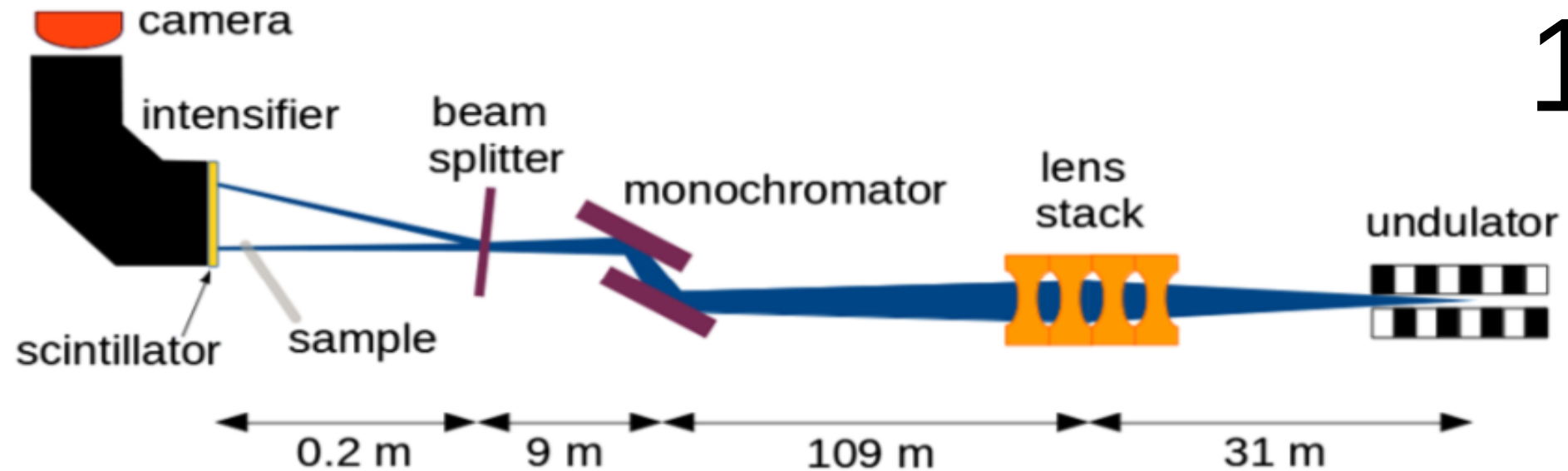
<sup>5</sup>*Synchrotron Soleil, 91192 Gif-sur-Yvette, France*

<sup>6</sup>*Helmholtz-Zentrum Dresden-Rossendorf, 01328 Dresden, Germany*

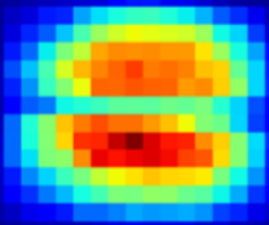
(Received 16 May 2016; published 7 September 2016)



10

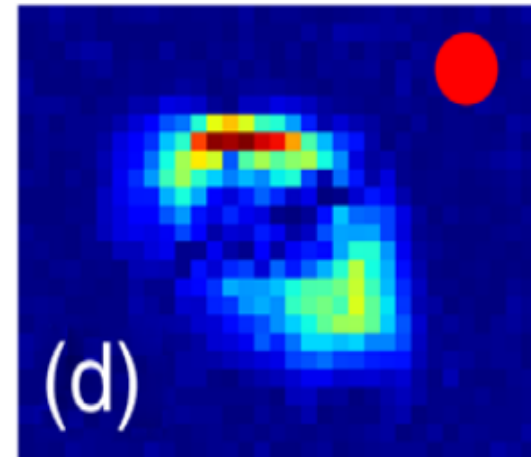


(c)



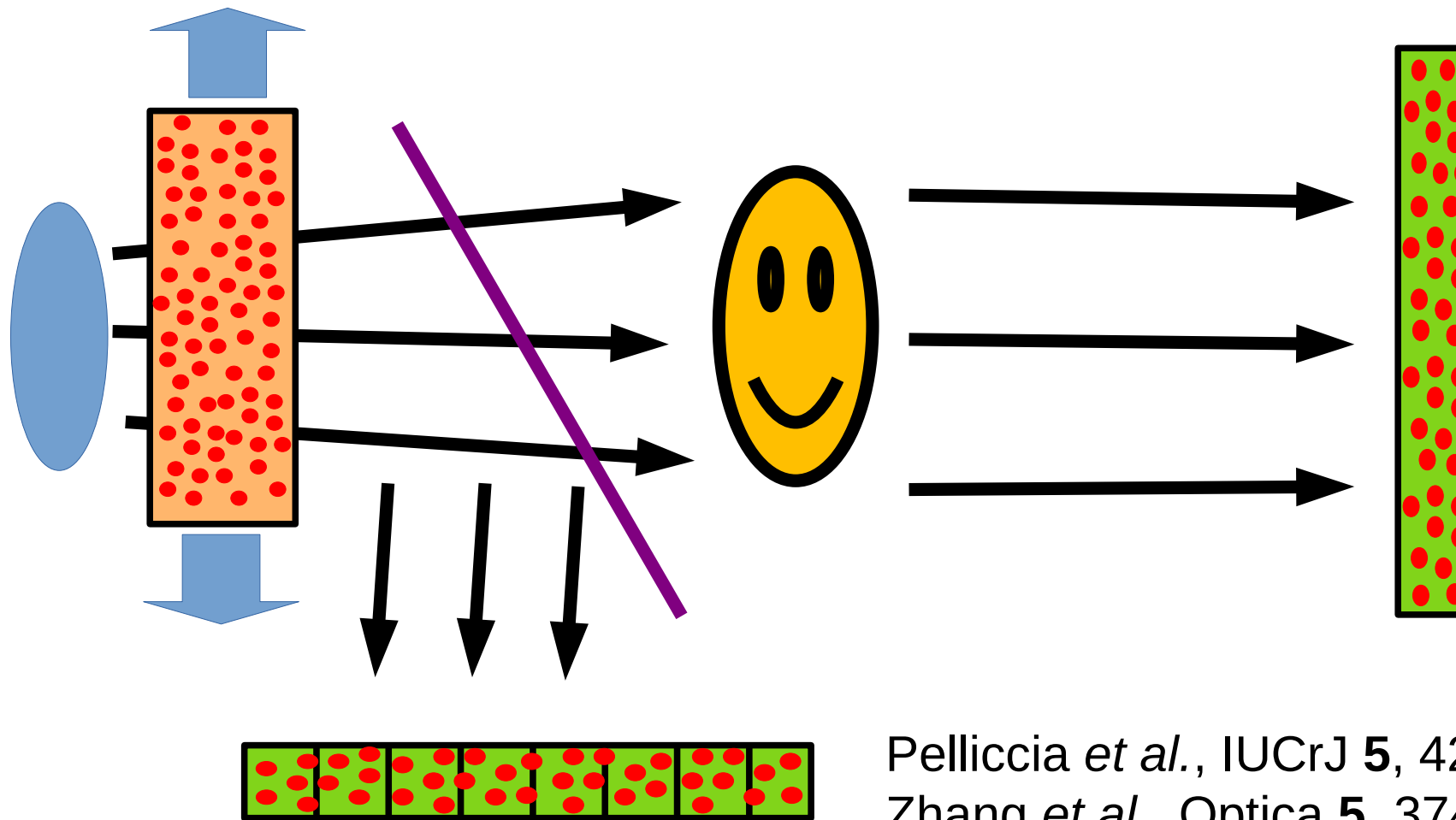
Pelliccia, Rack, Scheel,  
Cantelli & Paganin, Phys.  
Rev. Lett. **117**, 113902 (2016).

(d)



# X-ray ghost imaging, version two of two

12



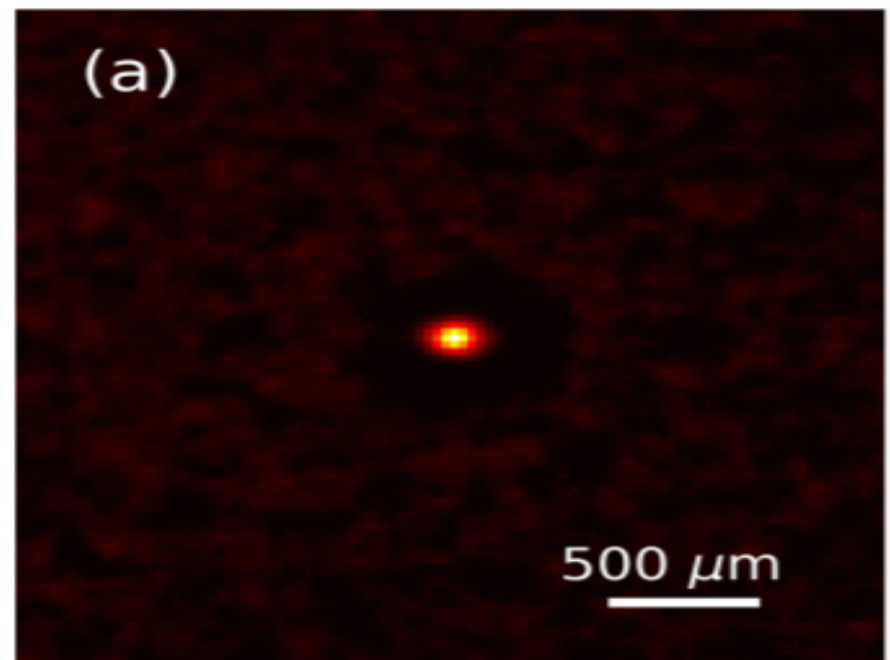
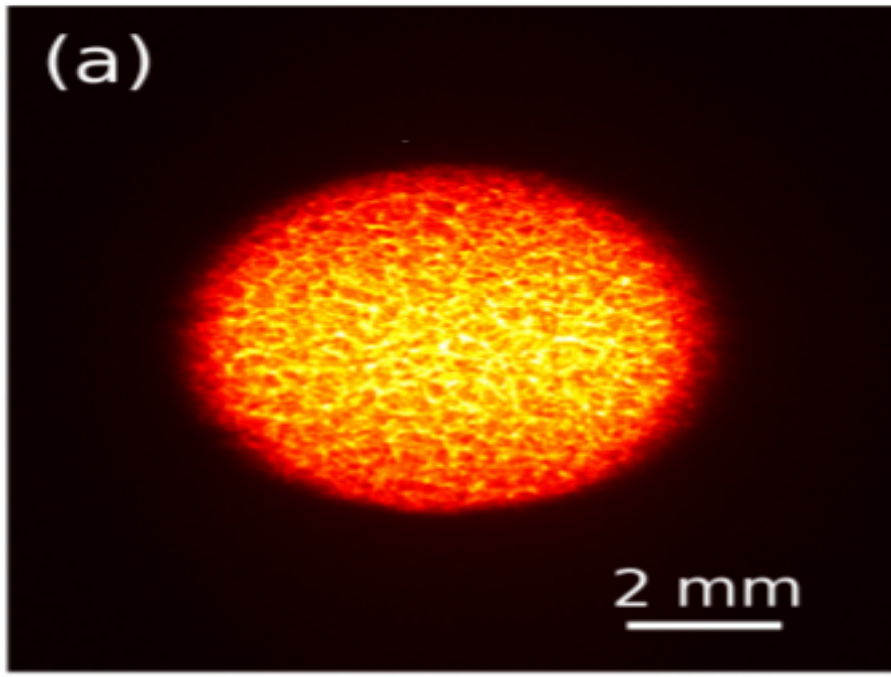
Pelliccia *et al.*, IUCrJ 5, 428 (2018)  
Zhang *et al.*, Optica 5, 374-377 (2018)

$$\text{PSF}(x - x', y - y') = \frac{1}{m} \sum_{j=1}^m [I_j(x', y') - \bar{I}] [I_j(x, y) - \bar{I}].$$

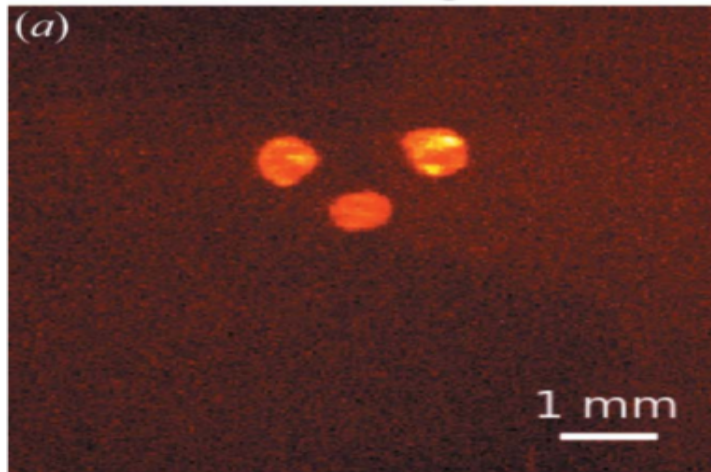
13

$$v(x, y) * \text{PSF}(x, y) = \frac{1}{m} \sum_{j=1}^m (b_j - \bar{b}) I_j(x, y)$$

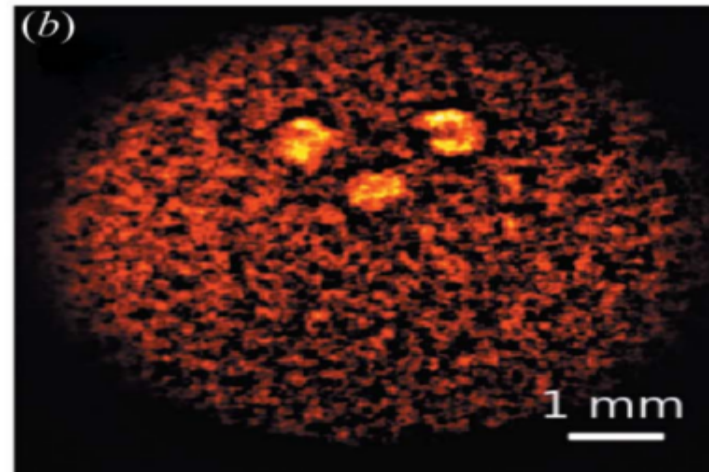
cf. Bromberg et  
al., Phys. Rev. A,  
79, 053840 (2009).



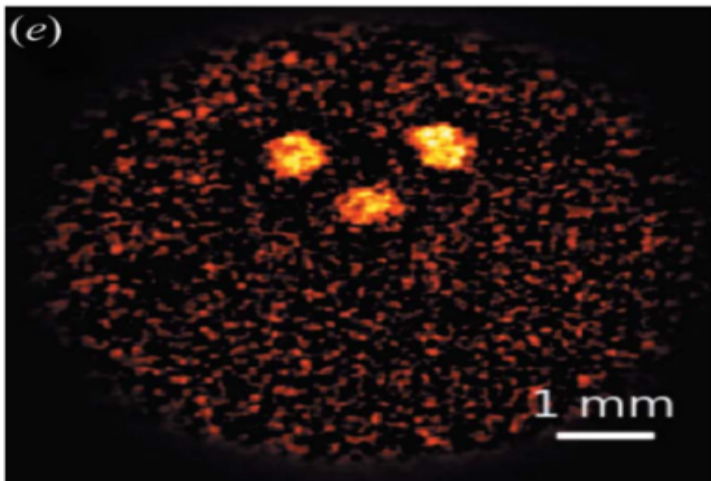
Direct image



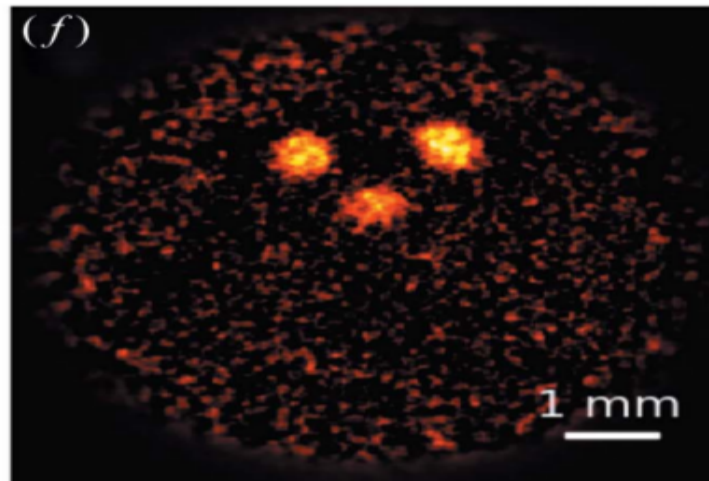
Conventional GI



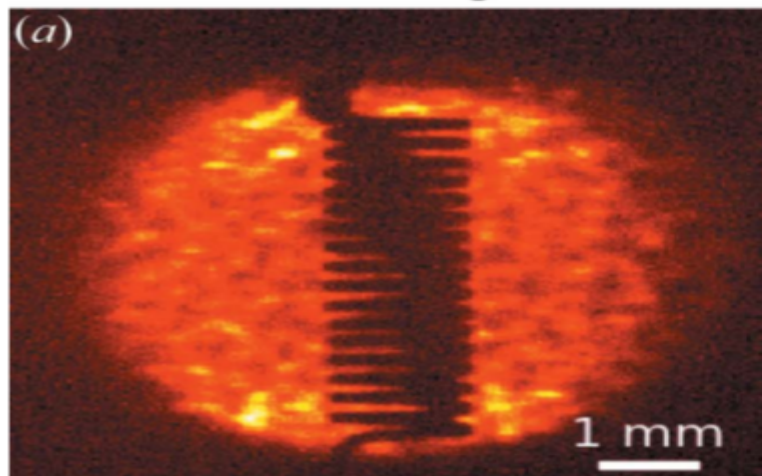
50 Landweber iterations



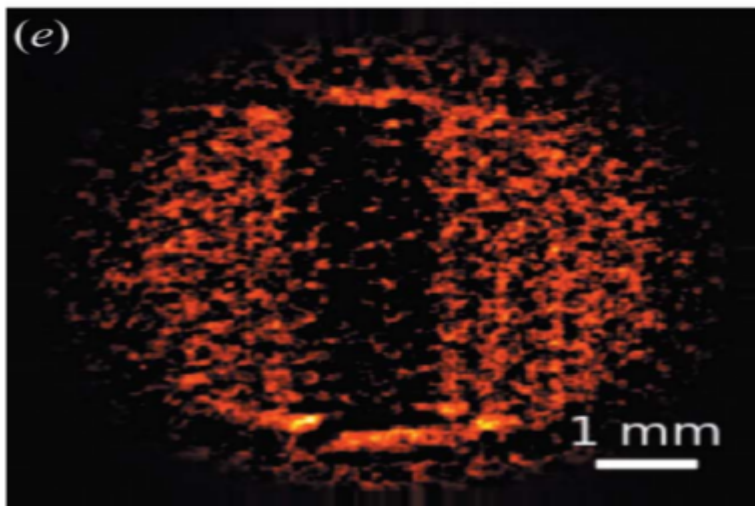
150 Landweber iterations



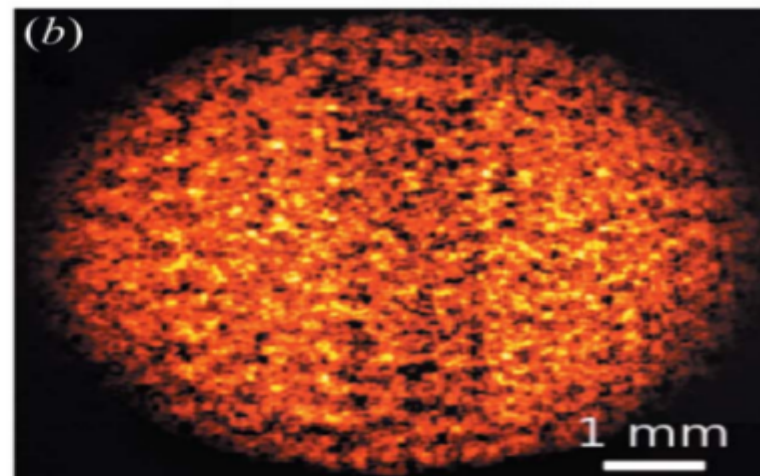
Direct image



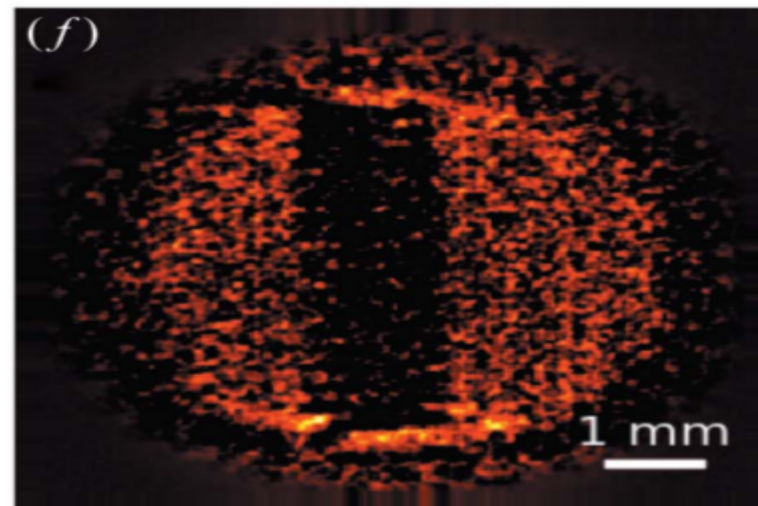
100 Landweber iterations

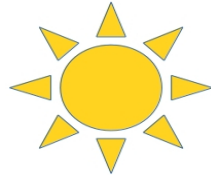


Conventional GI

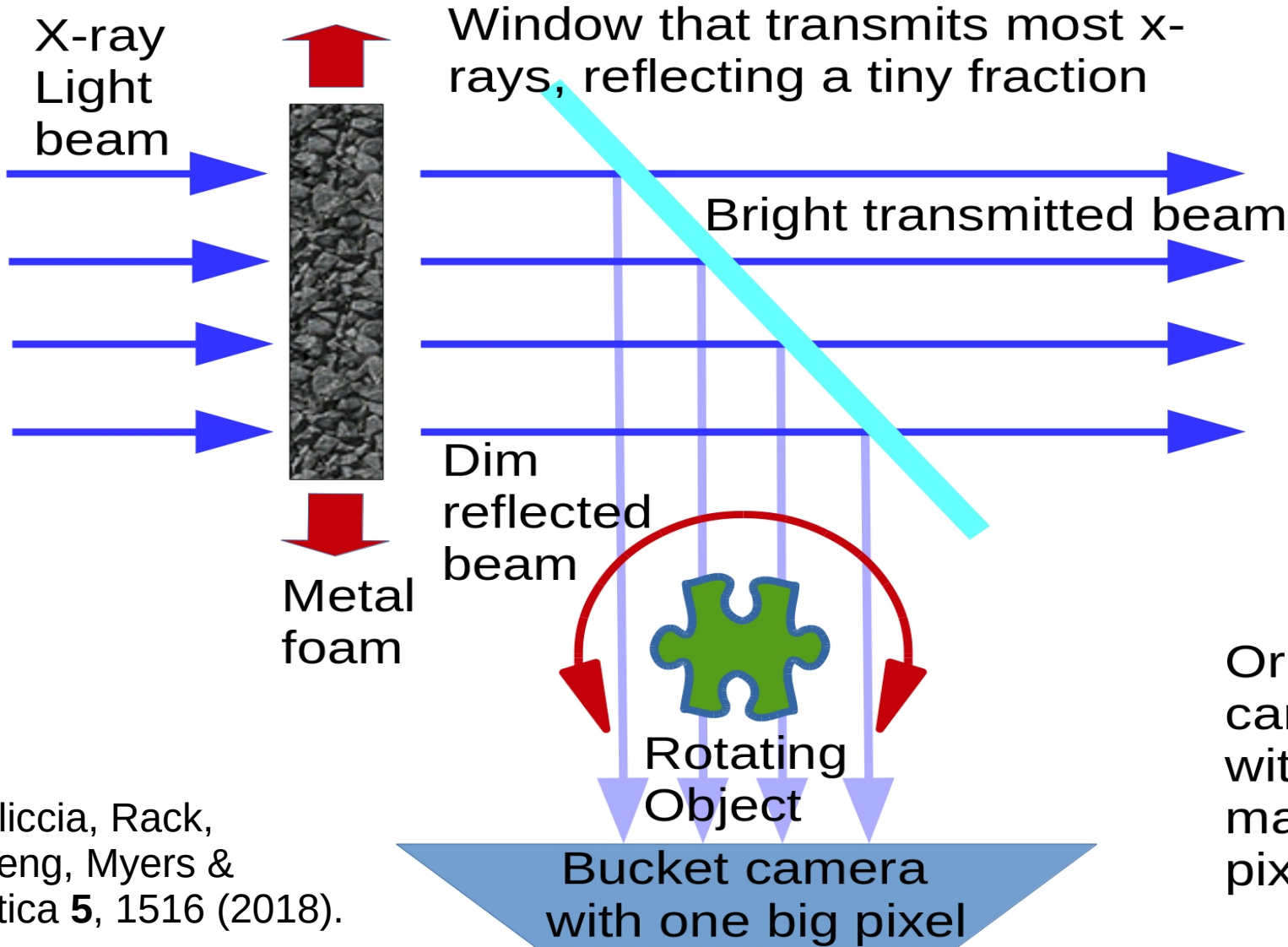


250 Landweber iterations

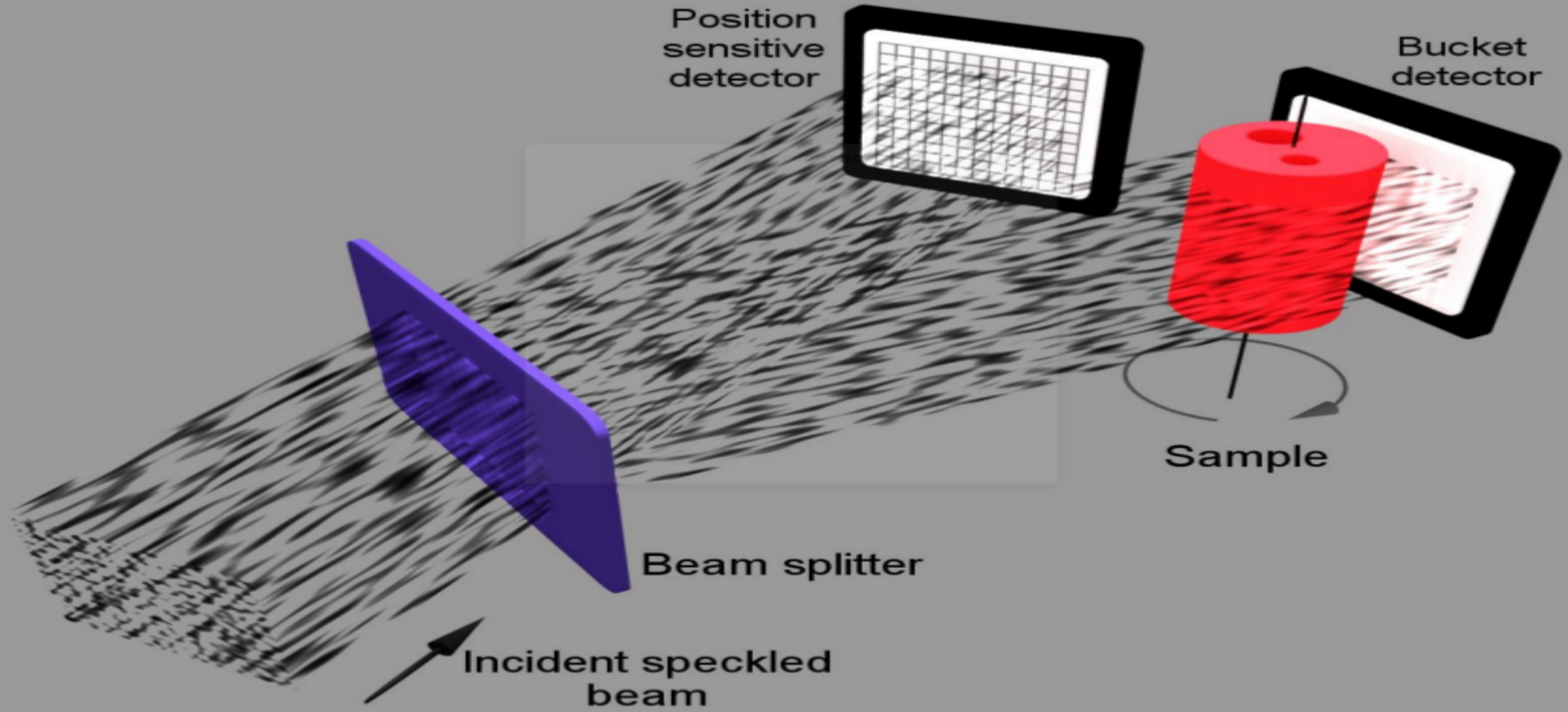




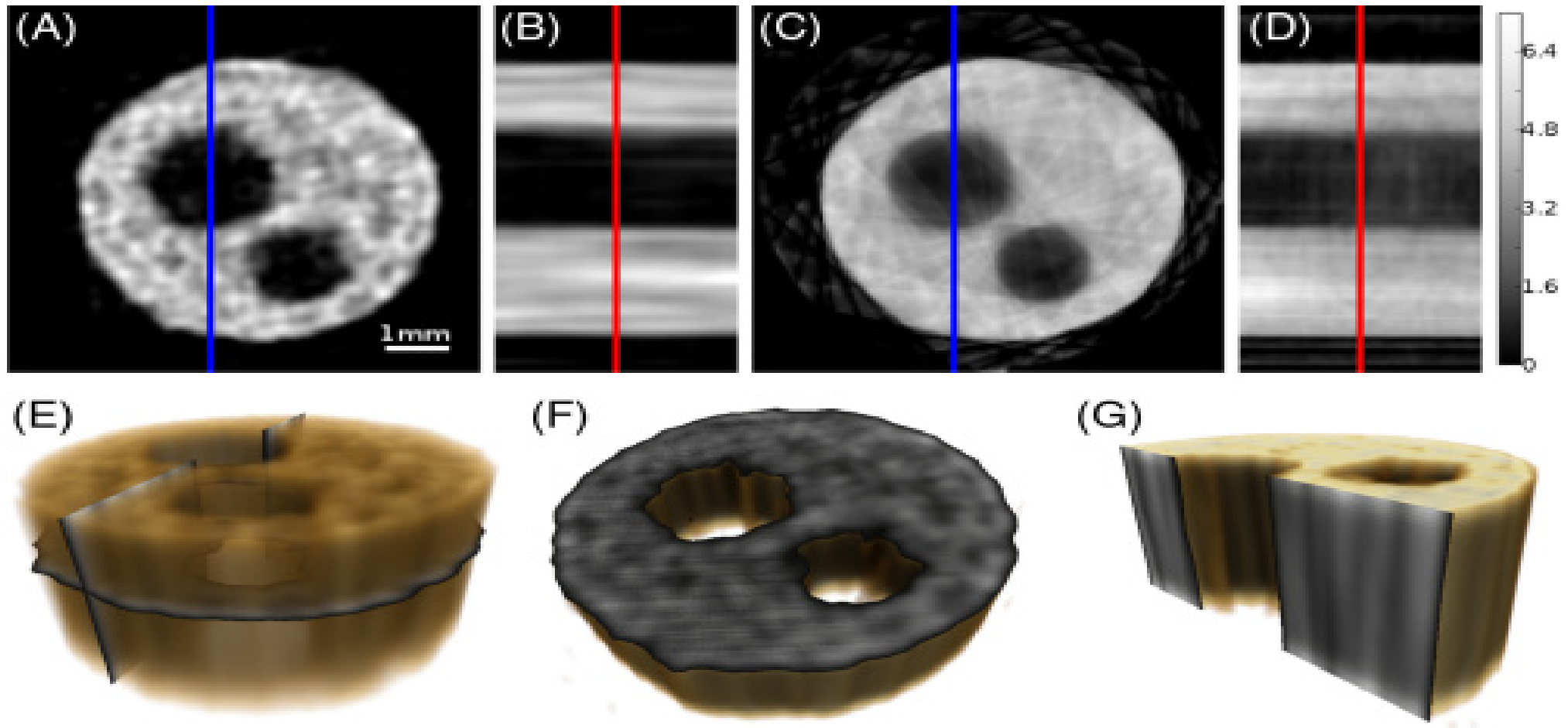
X-ray source



Kingston, Pelliccia, Rack,  
Olbinado, Cheng, Myers &  
Paganin, Optica 5, 1516 (2018).



Kingston, Myers, Pelliccia, Svalbe & Paganin, IEEE Trans. Comp. Imaging 5, 136 (2019).  
Kingston, Pelliccia, Rack, Olbinado, Cheng, Myers, Paganin, Optica 5, 1516 (2018).



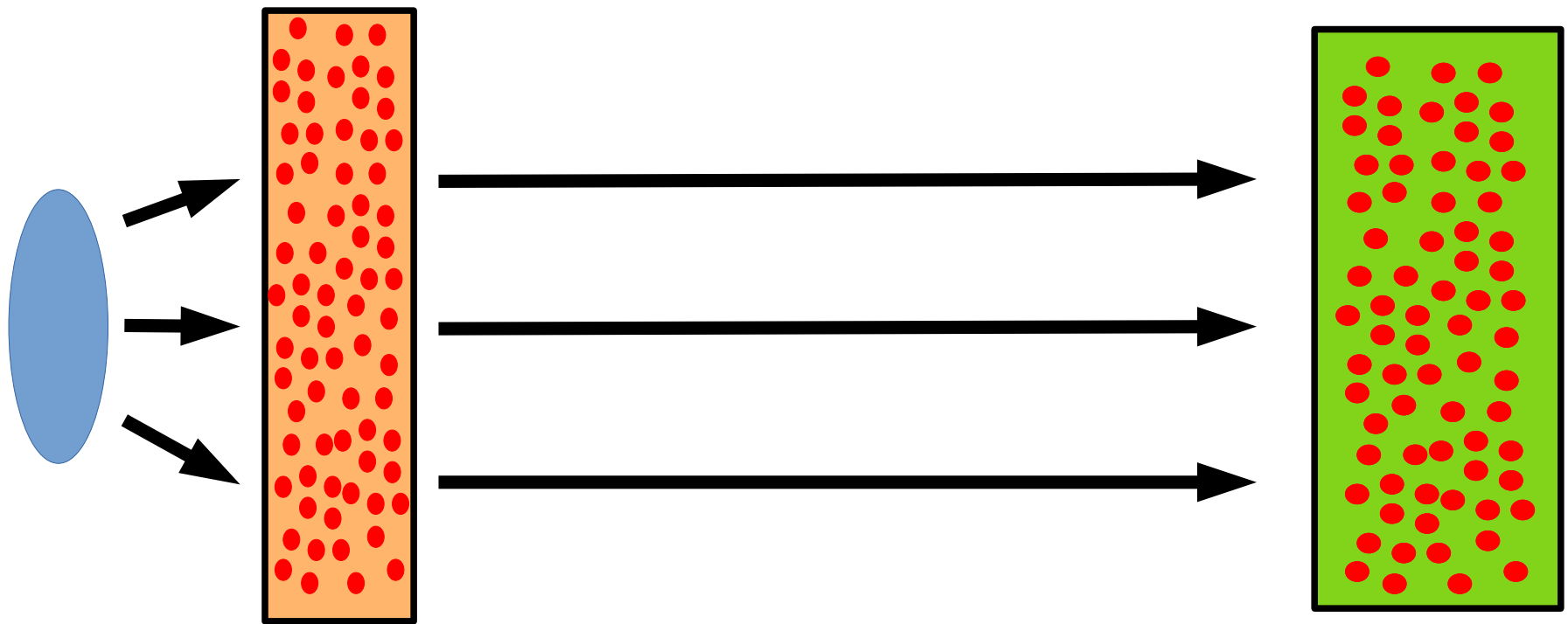
Kingston, Pelliccia, Rack, Olbinado, Cheng,  
Myers & Paganin, Optica 5, 1516 (2018).

“Bucket detectors  
are bad because...”

“Bucket detectors  
are good because...”

Hybrid virtual-actual optics ... computer as an intrinsic part of imaging system ... tomographers doing this for long time ... replace hardware with software ... computing power cheap, throw away more and more hardware ... including the position-sensitive detector .. spectroscopy ... fluorescence.

# Ghost projection

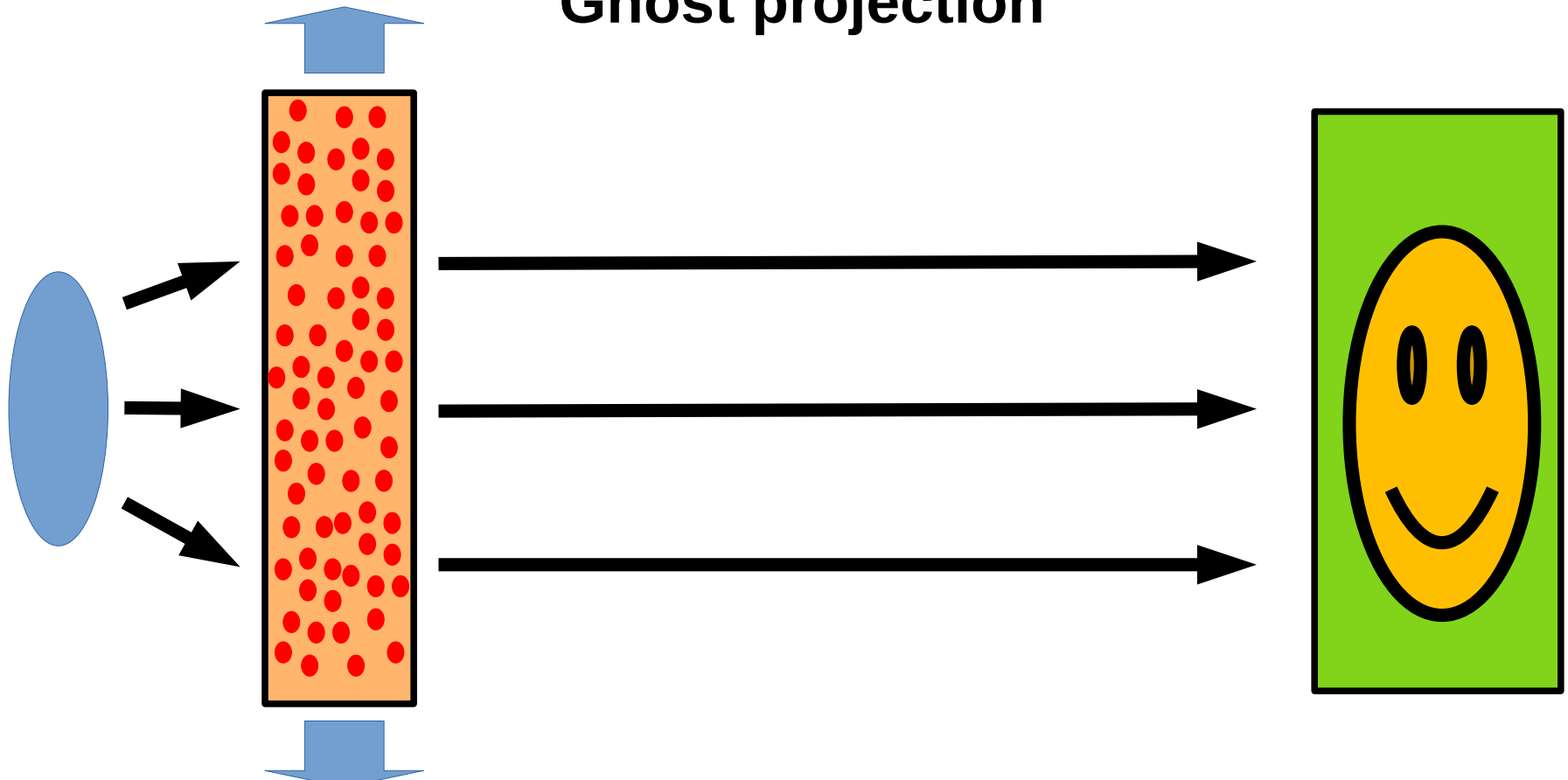


Paganin, Physical Review A **100**, 063823 (2019)

Ceddia & Paganin, Physical Review A **105**, 013512 (2022)

Ceddia, Kingston, Pelliccia, Rack & Paganin, arXiv:2202.10572 (2022)

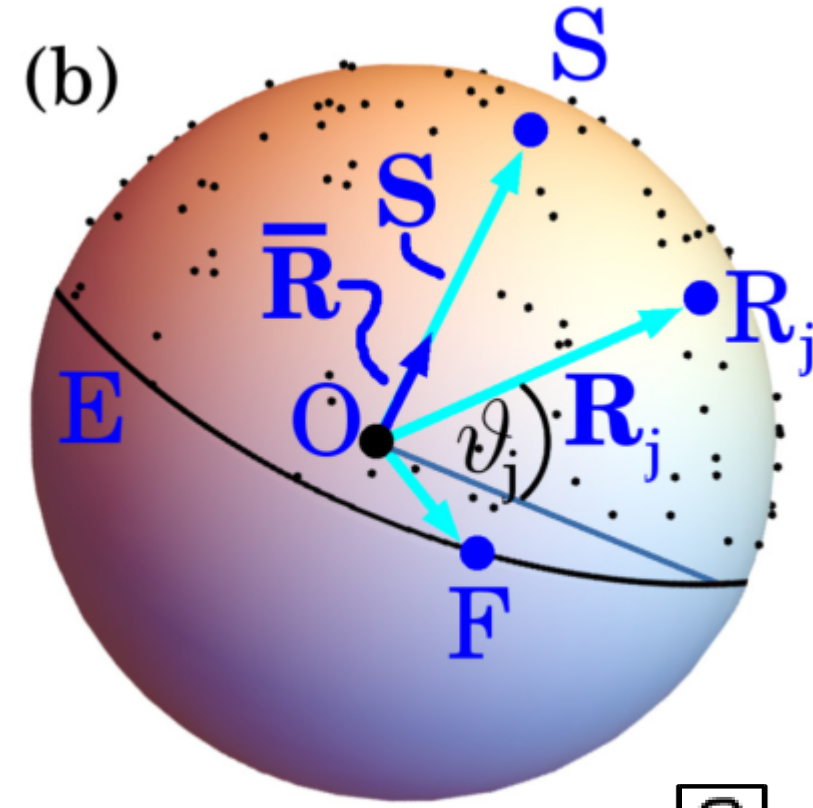
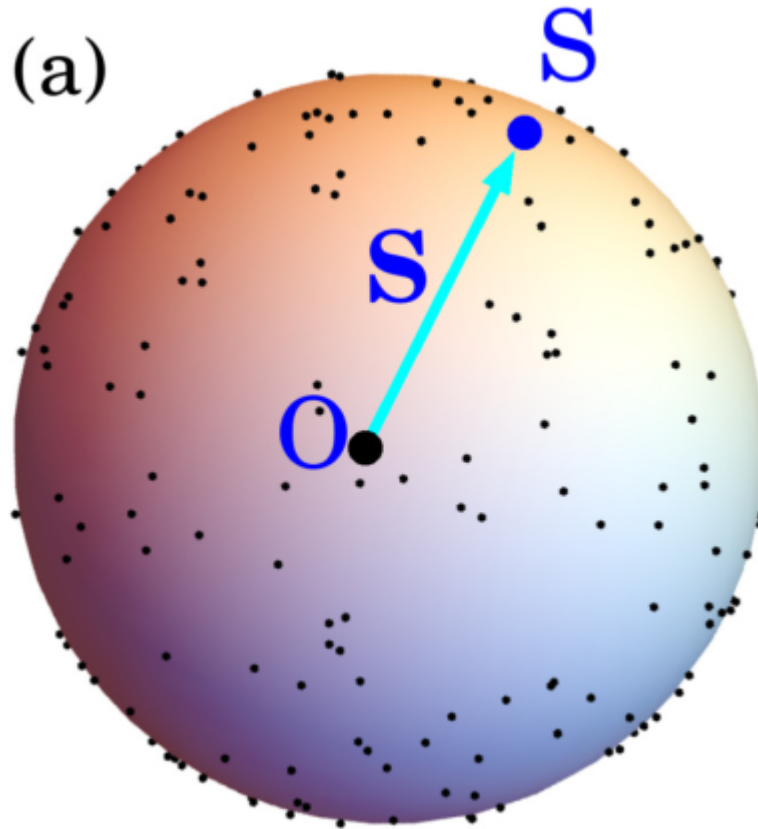
# Ghost projection



Paganin, Physical Review A **100**, 063823 (2019)

Ceddia & Paganin, Physical Review A **105**, 013512 (2022)

Ceddia, Kingston, Pelliccia, Rack & Paganin, arXiv:2202.10572 (2022)

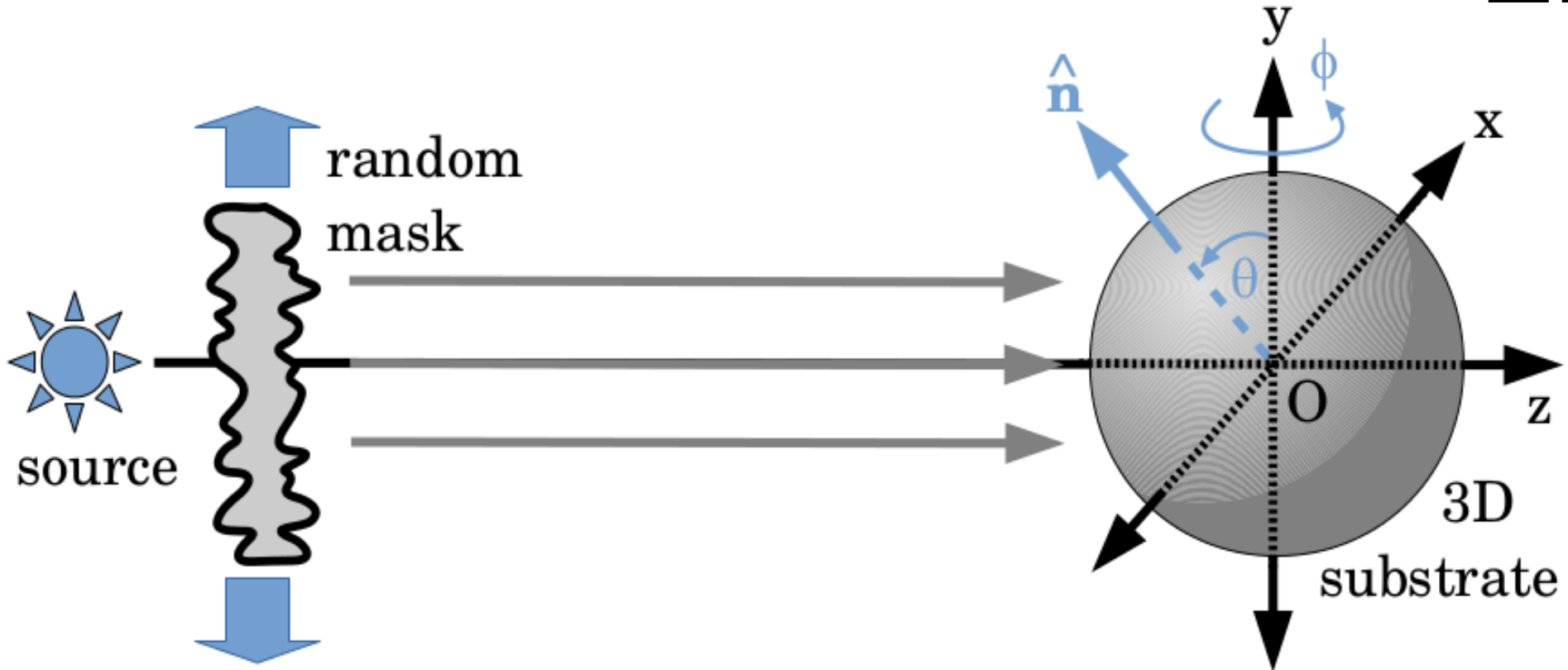


$$\begin{aligned} \text{[Icon]} &= a \text{ [QR code]} + b \text{ [QR code]} \\ &+ c \text{ [QR code]} + d \text{ [QR code]} + \dots \end{aligned}$$

D. M. Paganin, "Writing arbitrary distributions of radiant exposure by scanning a single illuminated spatially-random screen", Phys. Rev. A 100, 063823 (2019).

# GHOST TOMOGRAPHY IN REVERSE

22



D. M. Paganin, "Writing arbitrary distributions of radiant exposure by scanning a single illuminated spatially-random screen", Phys. Rev. A 100, 063823 (2019).

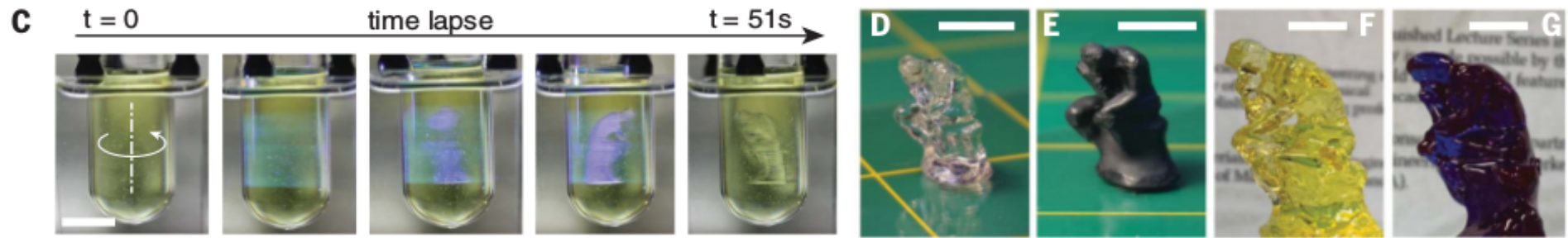
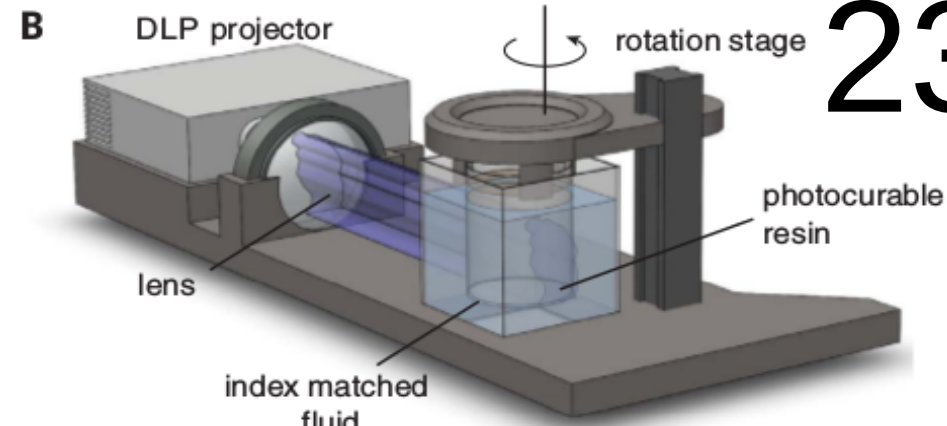
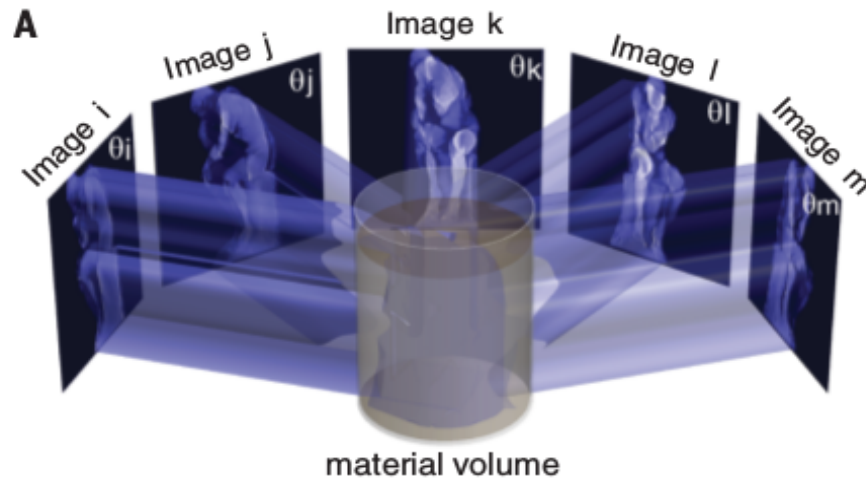
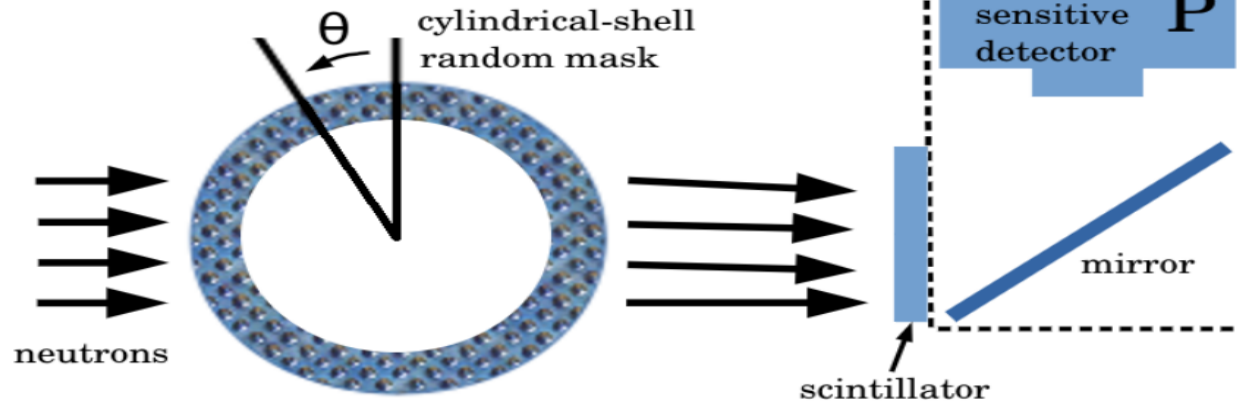
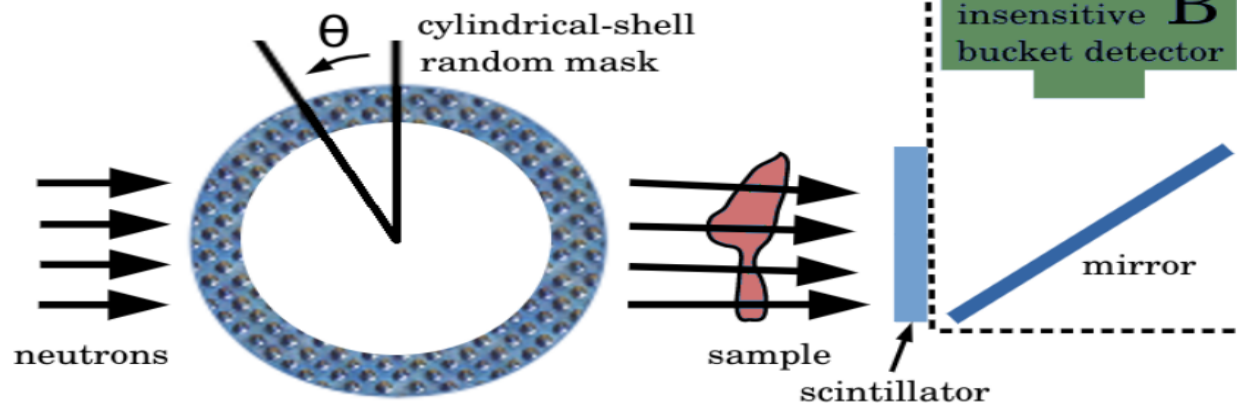


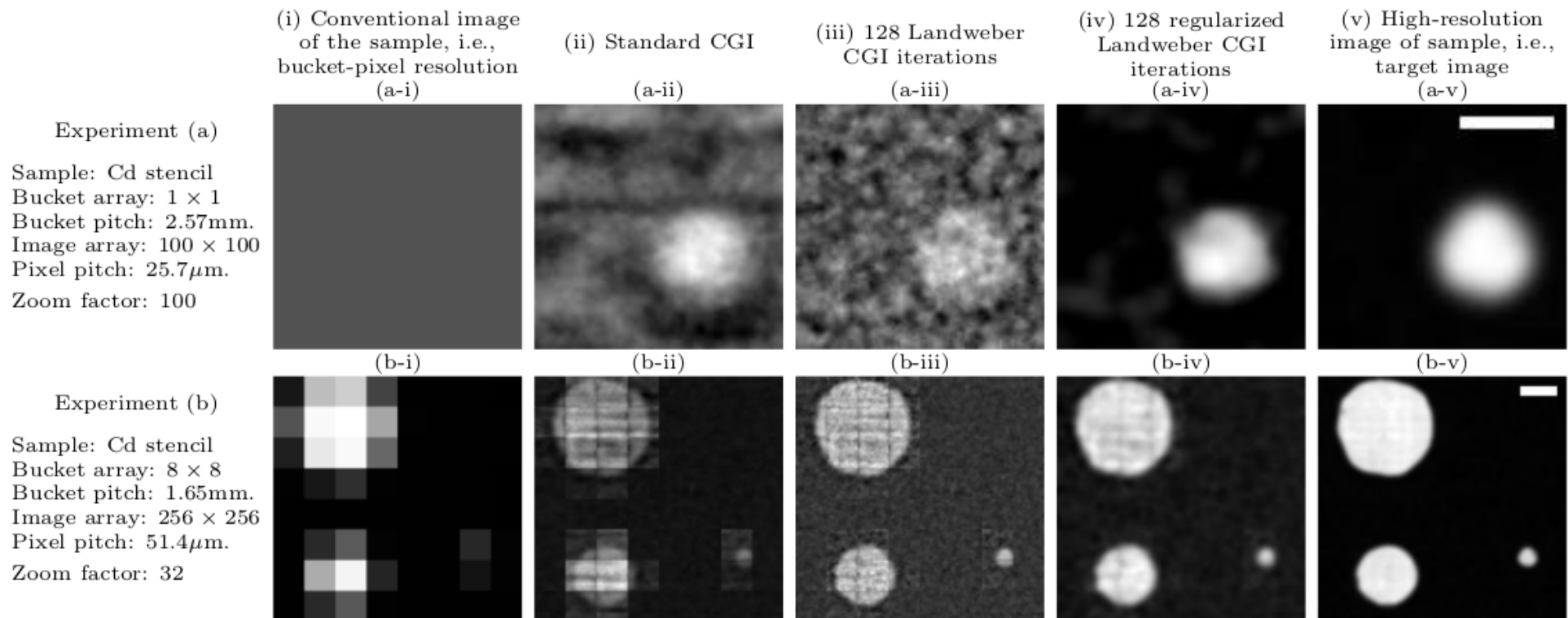
**Fig. 1 CAL volumetric fabrication.** **(A)** Underlying concept: Patterned illumination from many directions delivers a computed 3D exposure dose to a photoresponsive material. **(B)** Schematic of the CAL system used in this work. DLP projector, digital light processor-based projector. **(C)** Sequential view of the build volume during a CAL print. A 3D geometry is formed in the material in less than 1 min. **(D)** The 3D part shown in (C) after rinsing away uncured material. **(E)** The part from (D), painted for clarity. **(F)** A larger (40-mm-tall) version of the same geometry. **(G)** Opaque version of the geometry in (F), using crystal violet dye in the resin. Scale bars: 10 mm.

(a)



(b)





(i) Conventional image  
of the sample, i.e.,  
bucket-pixel resolution

(ii) Standard CGI

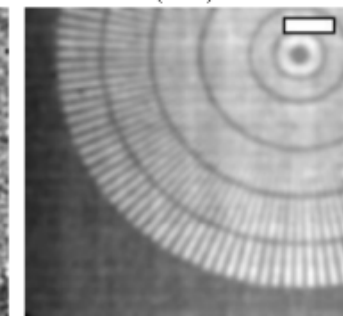
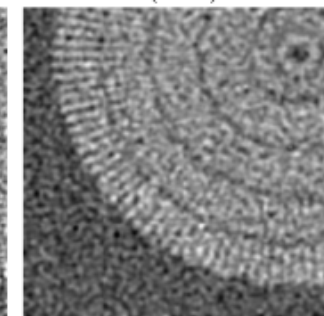
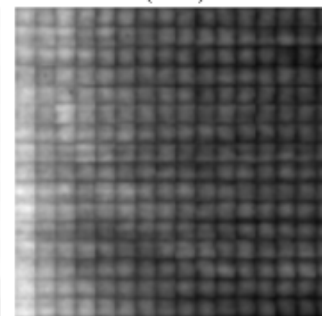
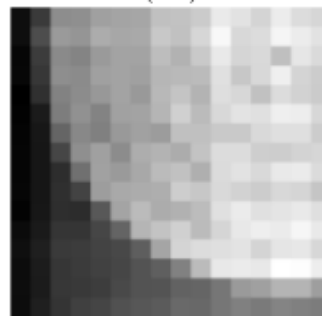
(iii) 128 Landweber  
CGI iterations

(iv) 128 regularized  
Landweber CGI  
iterations

(v) High-resolution  
image of sample, i.e.,  
target image

Experiment (c)

Sample: Res. star  
Bucket array:  $16 \times 16$   
Bucket pitch: 0.82mm.  
Image array:  $256 \times 256$   
Pixel pitch:  $51.4\mu\text{m}$ .  
Zoom factor: 16



Experiment (d)

Sample: Res. star  
Bucket array:  $32 \times 32$   
Bucket pitch: 0.41mm.  
Image array:  $256 \times 256$   
Pixel pitch:  $51.4\mu\text{m}$ .  
Zoom factor: 8

